Technical University of Crete

ΠΑΝΕΠΙΣΤΗΜΙΟ ΠΑΤΡΩΝ
UNIVERSITY OF PATRAS

Advances in colloid and biocolloid transport in porous media: particle size-dependent dispersivity and gravity effects

Constantinos V. Chrysikopoulos[1], Ioannis D. Manariotis[2] and Vasiliki I. Syngouna[2]

[1]*School of Environmental Engineering, Technical University of Crete, Greece.*
[2]*Department of Civil Engineering, University of Patras, Greece*

EGU2014
HS8.1.7

BioNFate

Part A: Particle size-dependent dispersivity

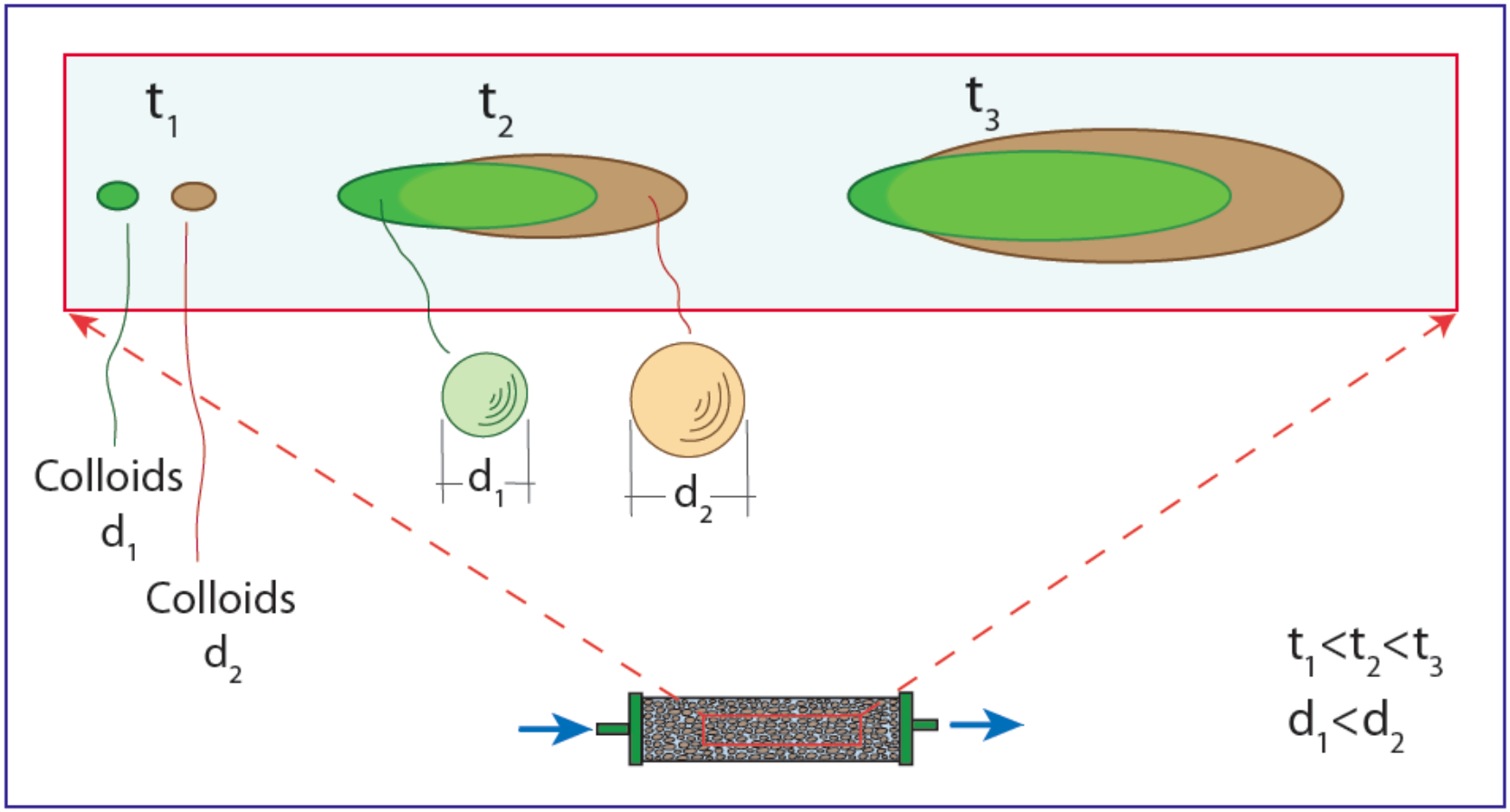

Previous studies

Early breakthrough of colloids as compared to conservative tracers

"Larger colloids are restricted by the size exclusion effect from sampling all paths"

Toran and Palumbo,1992
Powelson et al., 1993
Grindrod et al., 1996
Dong et al., 2002
Keller et al., 2004.
Vasiliadou and Chrysikopoulos, 2011
Sinton et al., 2012

Effective dispersion in a uniform fracture

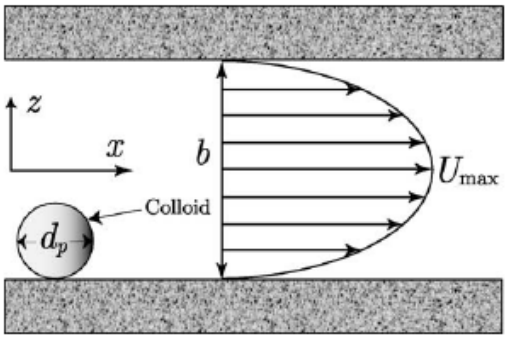

$$D_{\text{eff}} = \mathcal{D} + \frac{2}{945}\frac{U_{\max}^2 b^2}{\mathcal{D}}\left(1 - \frac{d_p}{b}\right)^6$$

$$D_{\text{Taylor}} = \mathcal{D} + \frac{2}{945}\frac{U_{\max}^2 b^2}{\mathcal{D}}$$

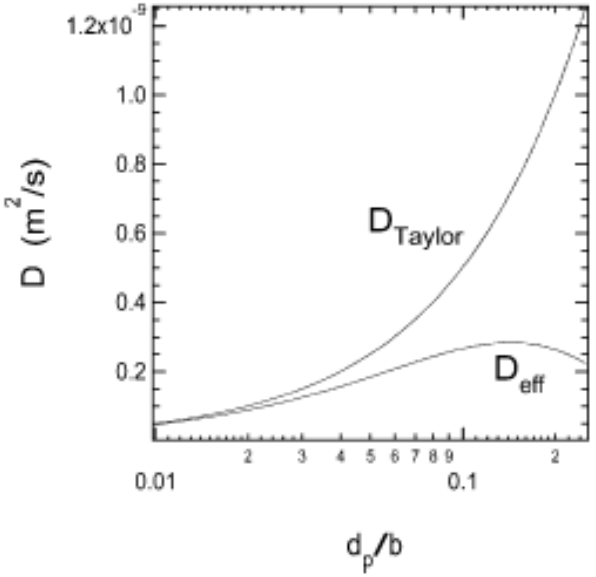

James and Chrysikopoulos, *J. Colloid and Interface Science*, 2003.

Early work on particle size-dependent dispersivity

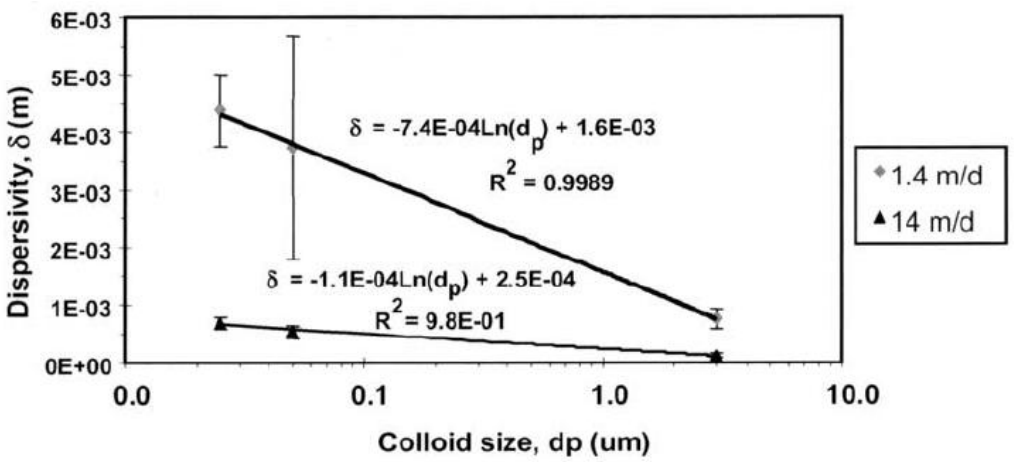

Mass recovered: M_r = 28.8 to 41.0 %
(size exclusion effect)

Keller, A.A., S. Sirivithayapakorn, and C.V. Chrysikopoulos, *Water Resources Research*, 2004.

Materials and methods

Columns: diameter = 2.5 cm
length = 15 & 30 cm
packed with glass beads (d_c=1 or 2 mm)
placed horizontally to minimize gravity effects

Colloids: fluorescent polystyrene microspheres
d_p= 28, 100, 300, 600, 1000, 1750, 2100, 3000 and 5000 nm
C_o =10^7 - 10^{13} particles/mL
fluorescence spectrophotometry

Tracer: bromide in the form of NaBr (10^{-5} M)
ion chromatography

d_p/d_c: <0.0025
below the straining and wedging threshold of
>0.004 (*Johnson et al.*, 2010) or
>0.003 (*Bradford and Bettahar*, 2006)

Transport experiments were performed under unfavorable colloid attachment conditions.
Experimental data fitted with ColloidFit.

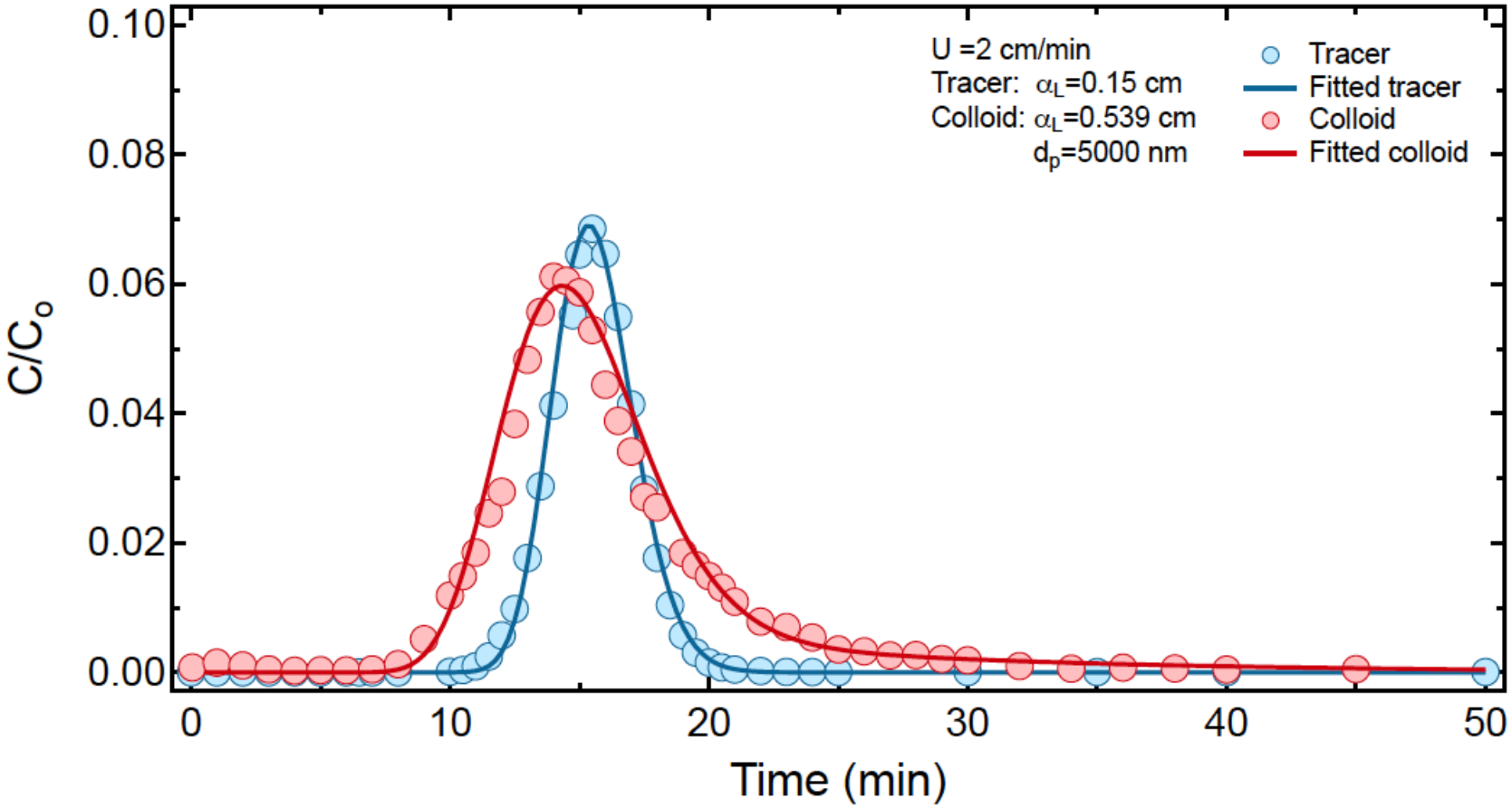

Figure A1. Early breakthrough

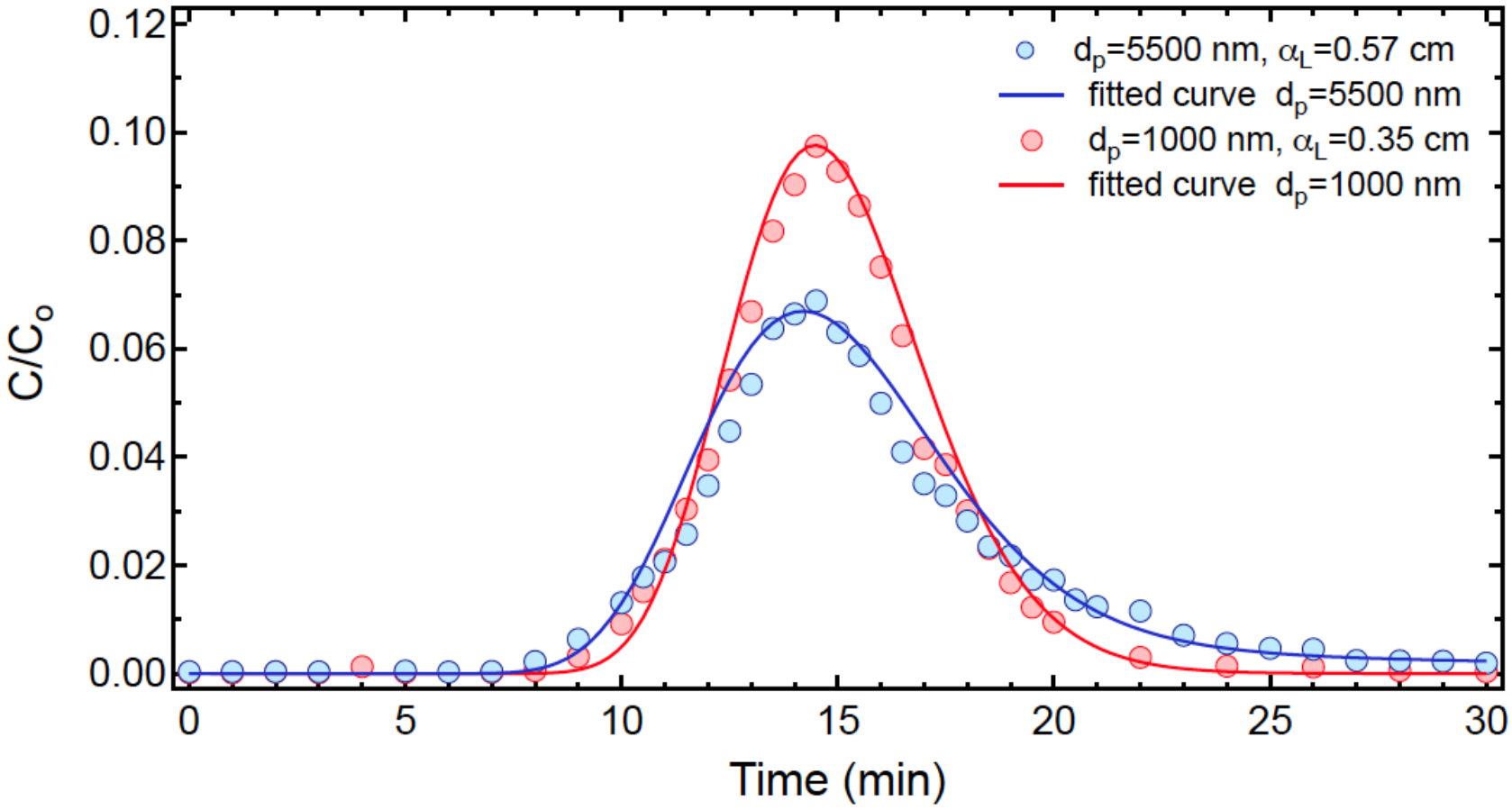

Figure A2. Breakthrough curves for two different colloids

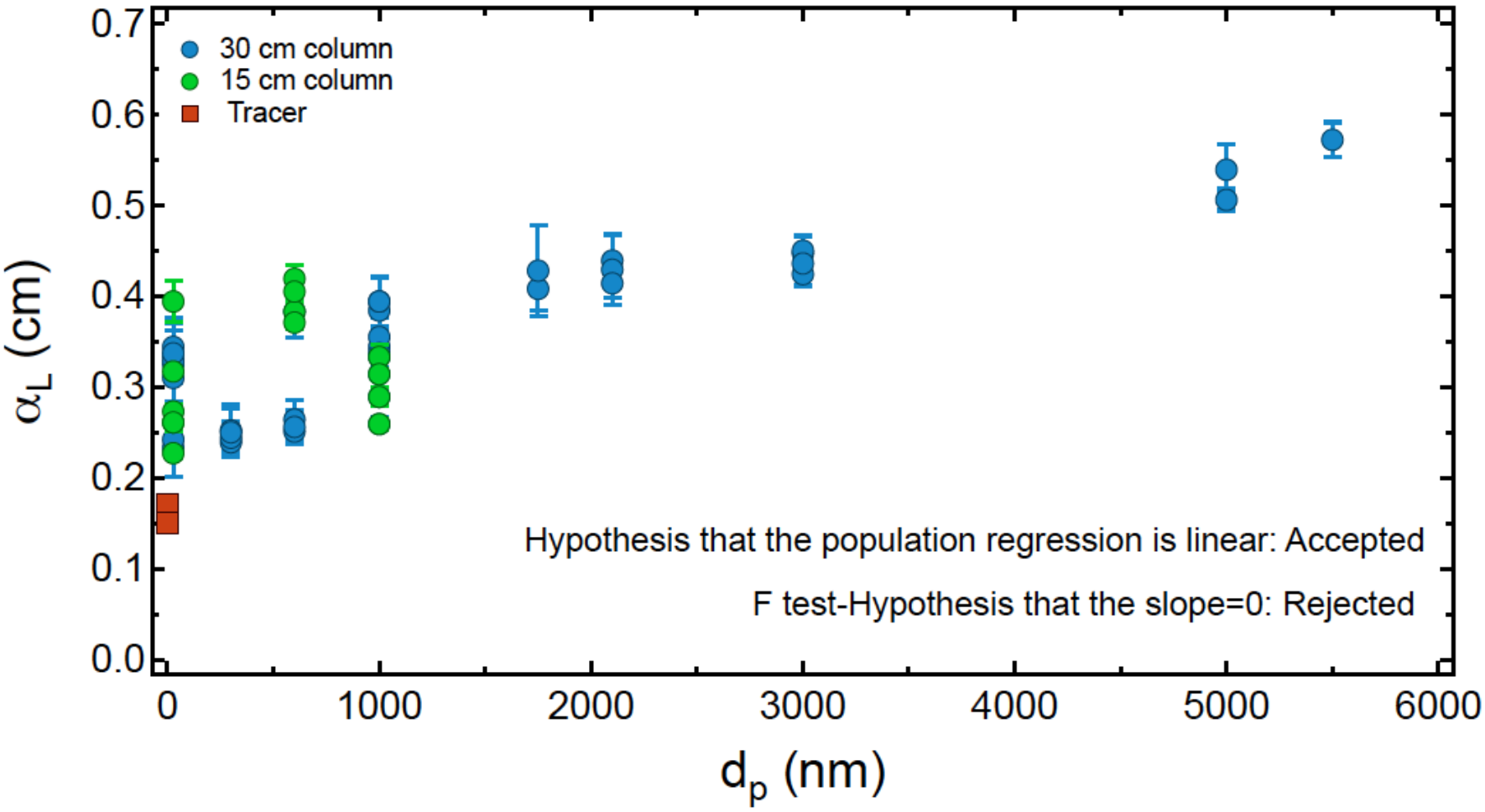

Figure A2. Longitudinal dispersivity as a function of colloid diameter.

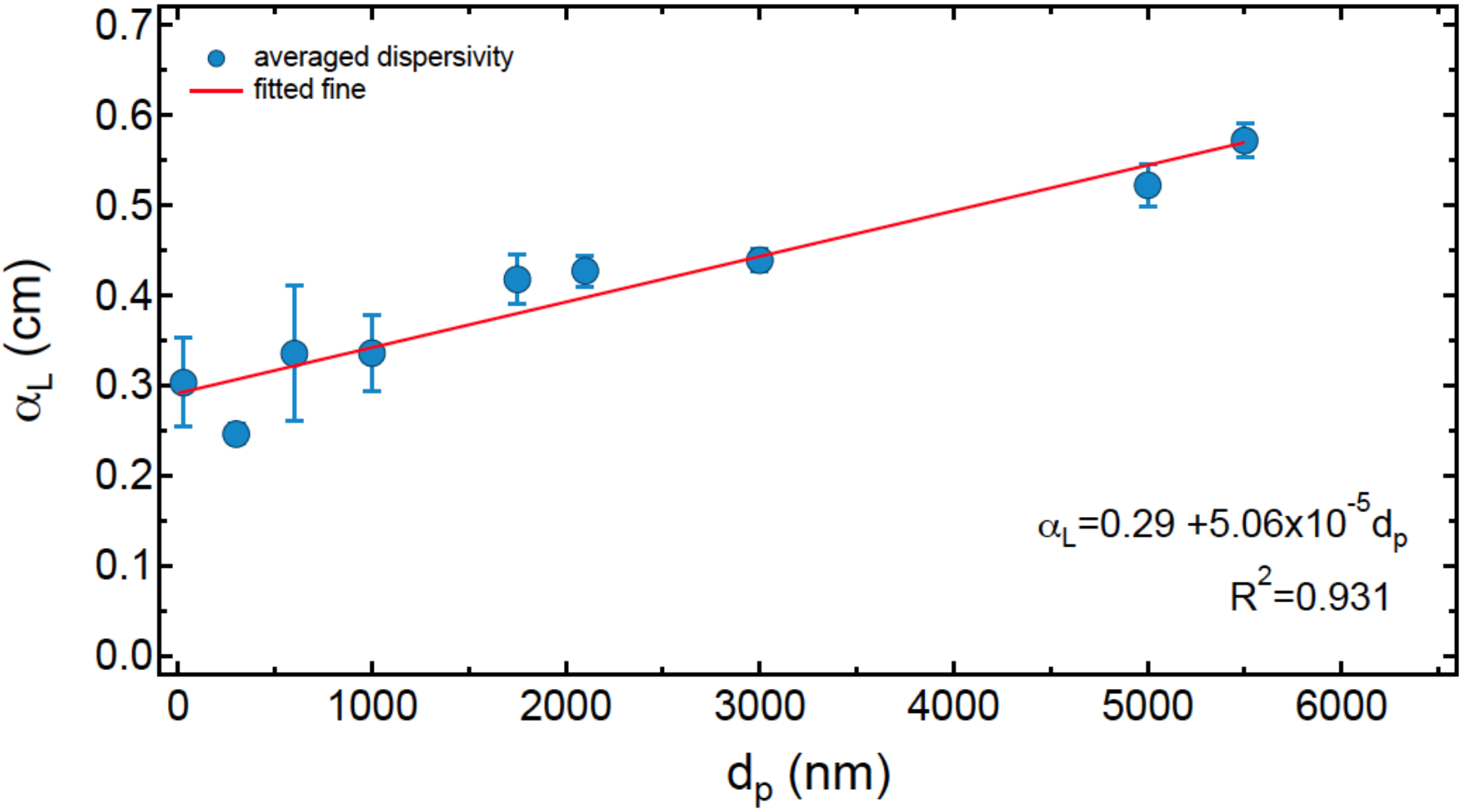

Figure A3. Longitudinal dispersivity (averaged) as a function of colloid diameter.

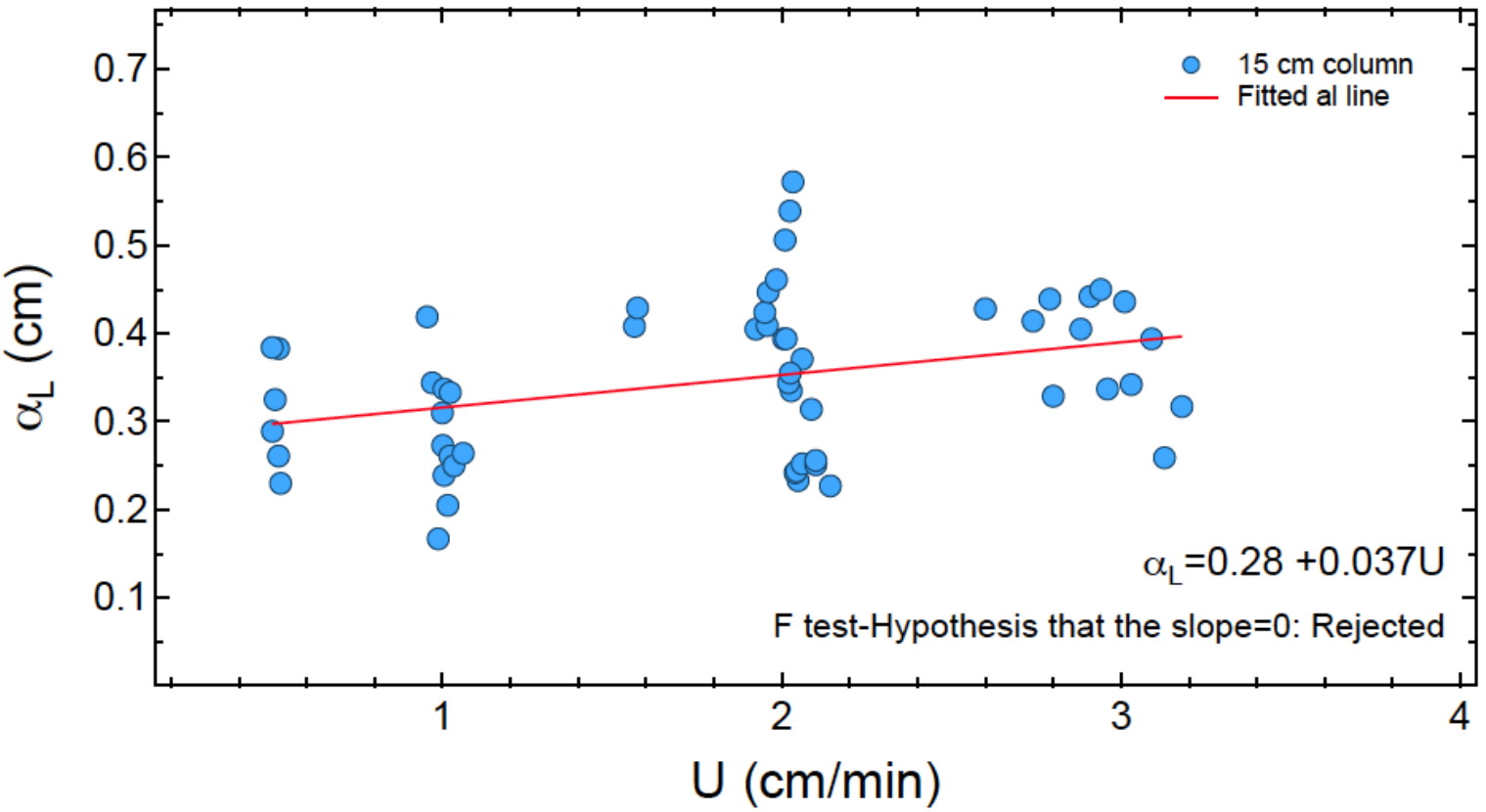

Figure A4. Longitudinal dispersivity as a function of interstitial velocity

Moment Analysis

Absolute temporal moments

$$m_n(L) = \int_0^\infty t^n C(L,t)\ dt$$

m_0 [tM/L^3]: total mass in the concentration distribution curve

m_1 [t^2M/L^3]: mean residence time

Normalized temporal moments

$$M_n(L) = \frac{m_n(L)}{m_0(L)} = \frac{\int_0^\infty t^n C(L,t)dt}{\int_0^\infty C(L,t)dt}$$

M_1 [t]: center of mass of the concentration distribution curve (defines the average velocity)

Mass recovery

$$M_r(L) = \frac{m_0(L)}{C_0 t_p}$$

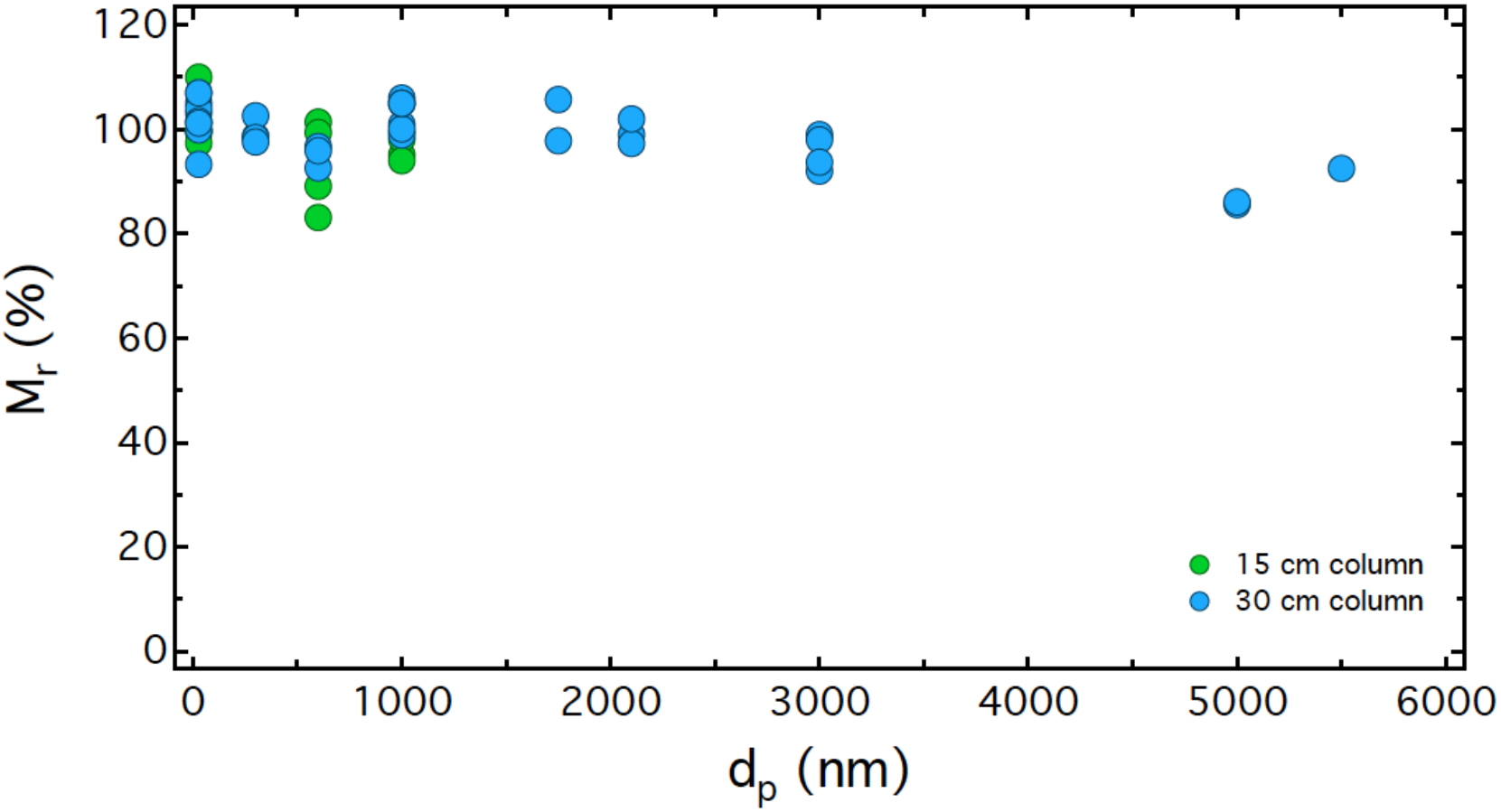

Figure A5. Mass recovery as a function of particle size

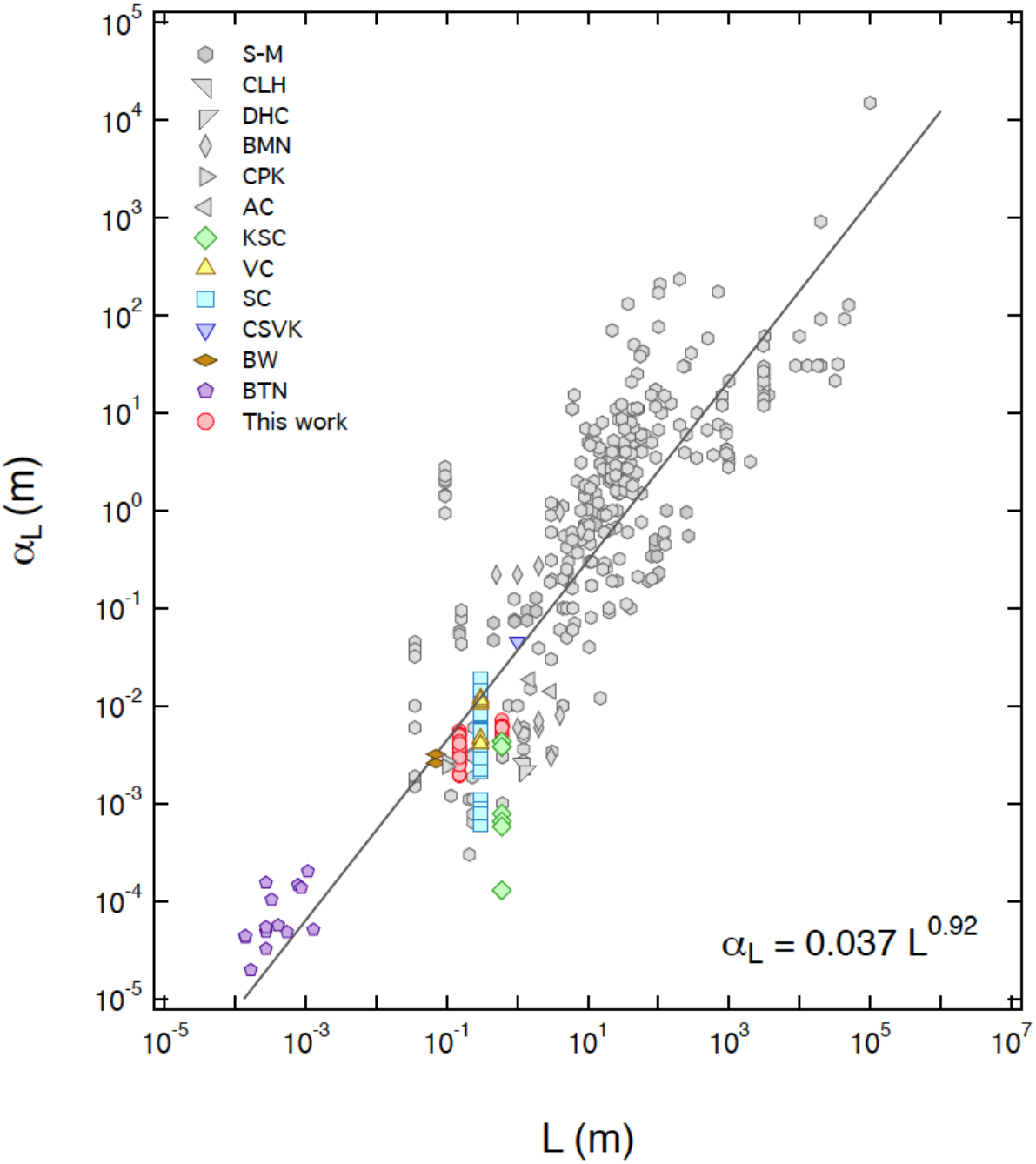

Figure A6. Compilation of 467 longitudinal dispersivities as a function of length scale. Molecular sized solutes are represented by gray symbols, and colloids/biocolloids by various colored symbols. The solid line is a standard linear regression line.

References

S-M [*Schulze-Makuch*, 2005]
CLH [*Chrysikopoulos et al.*, 2000]
DHC [*Dela Barre et al.*, 2002]
BMN [*Baumann et al.*, 2002]
CPK [*Chrysikopoulos et al.*, 2011]
AC [*Anders and Chrysikopoulos*, 2005]
KSC [*Keller et al.*, 2004]
VC [*Vasiliadou & Chrysikopoulos*, 2011]
SC [*Syngouna & Chrysikopoulos*, 2011]
CSVK [*Chrysikopoulos et al.*, 2012]
BW [*Bauman and Werth*, 2004]
BTN [*Baumann et al.*, 2010]

Results: Size-dependent dispersivity

- Colloid dispersivity increases with increasing colloid diameter.
- Early breakthrough is caused mainly by the increasing dispersivity.
- Fitted dispersion coefficients based on tracer data should not be used to analyze colloid experimental data.

Part B: Gravity effects

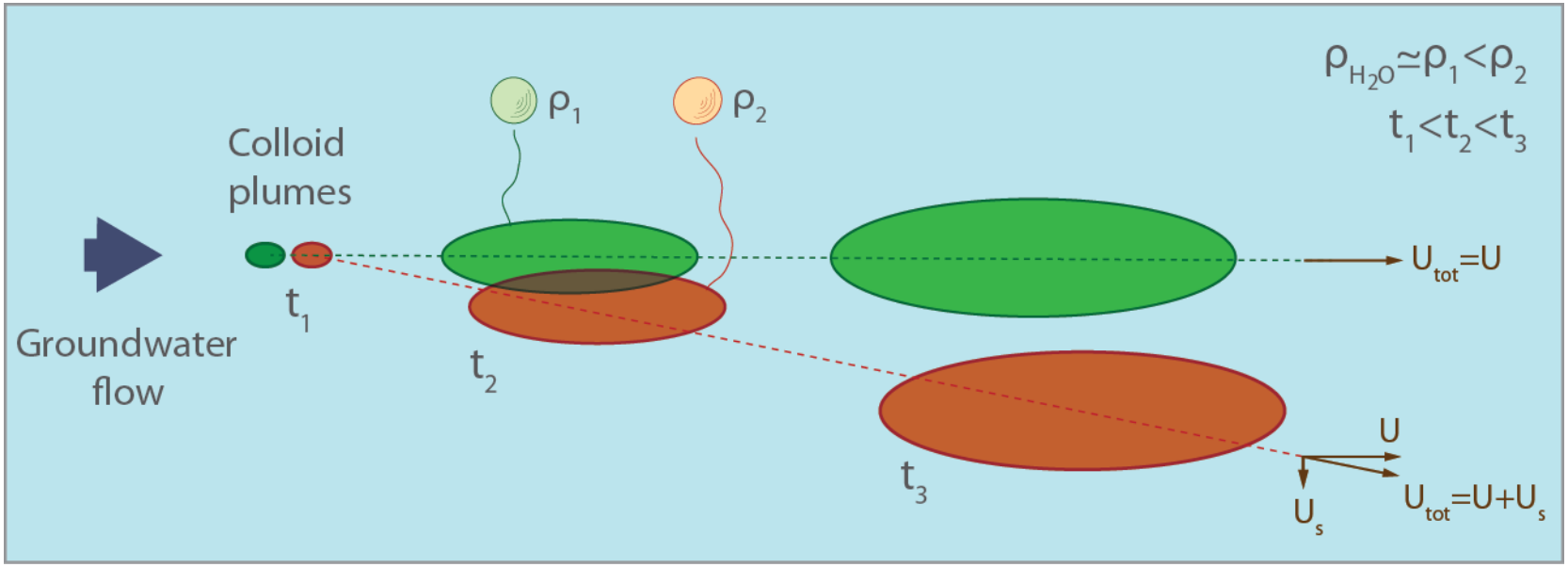

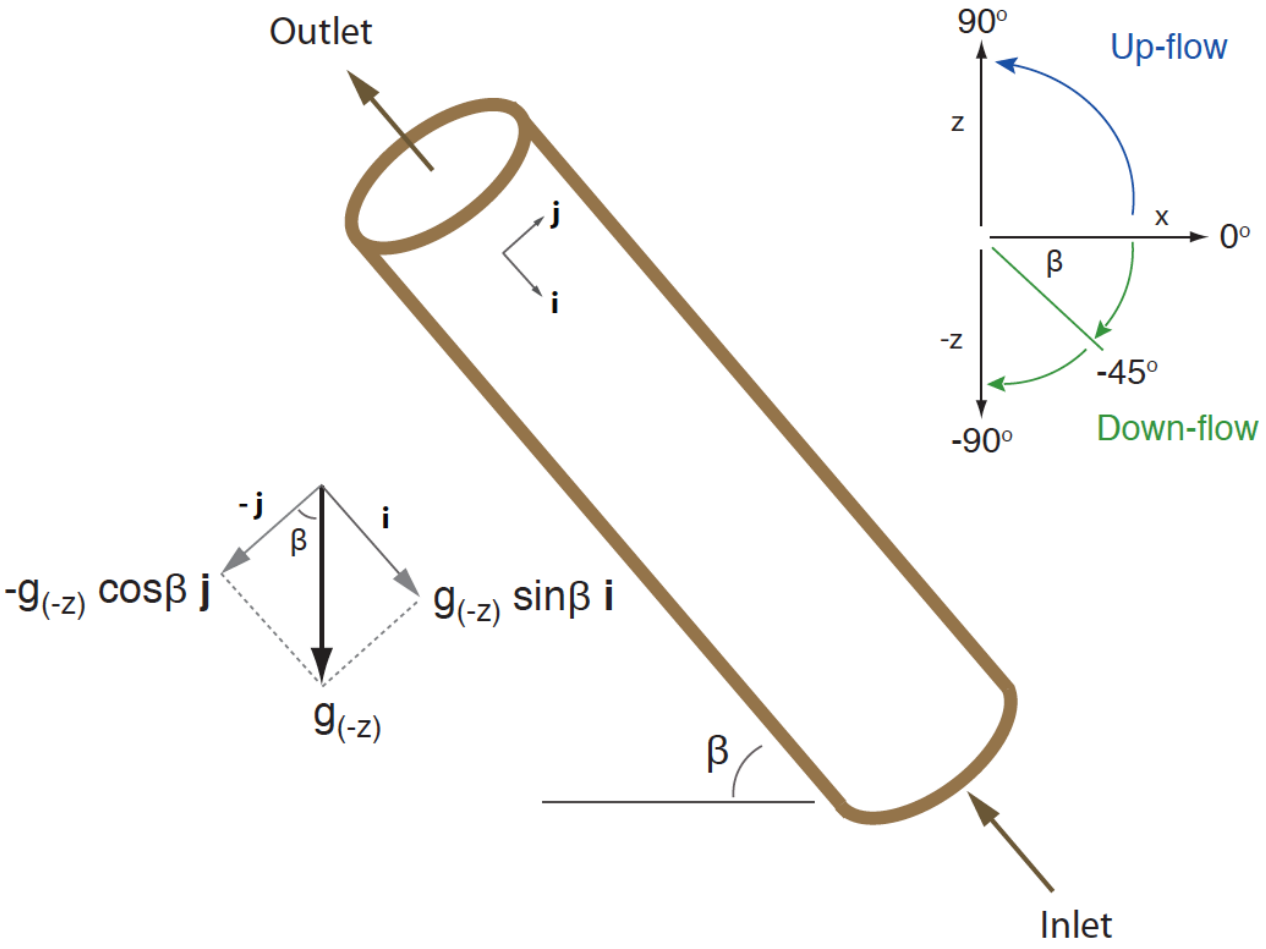

Figure B1. Schematic illustration of a packed column with up-flow velocity having orientation (**-i**) with respect to gravity. The gravity vector components are: $g_{(i)} = g_{(-z)}$ sinβ **i,** and $g_{(-j)} = -g_{(-z)}$ cosβ **j.**

“restricted particle” settling velocity

$$U_s = -f_s \frac{\left(\rho_p - \rho_w\right) d_p^2}{18\mu_w} g_{(\mathbf{i})}$$

$$g_{(\mathbf{i})} = g_{(-z)} \sin\beta \, \mathbf{i}$$

f_s [-] = correction factor accounting for particle settling in granular porous media (Wan et al., 1995)

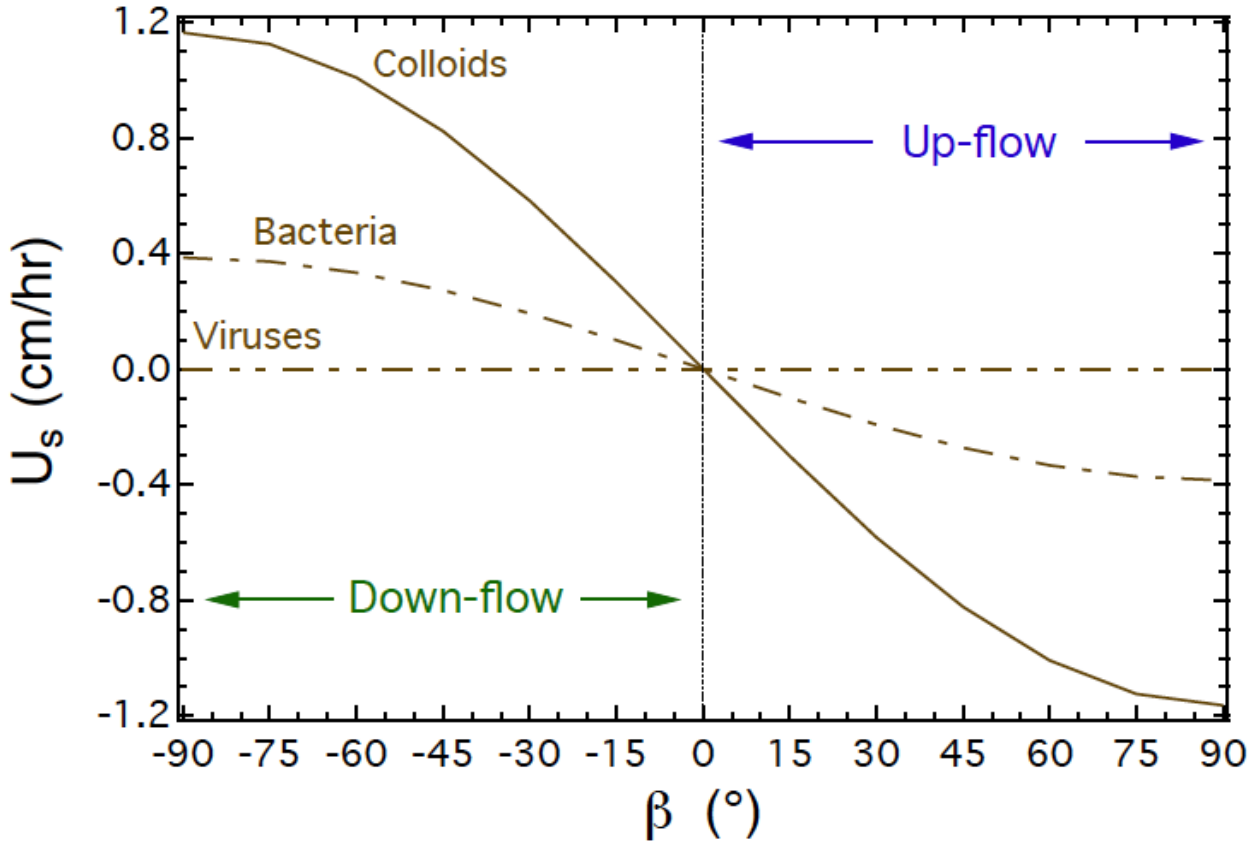

Figure B2. Restricted particle settling velocity as a function of column orientation and flow direction for colloids (clay: d_p=2 μm, ρ_p=2.65 g/cm^3), bacteria (*P. putida*: d_p=2.2 μm, ρ_p=1.45 g/cm^3), and viruses (MS2: d_p=25 nm, ρ_p=1.42 g/cm^3).

Mathematical Model

Governing transport equation

$$\frac{\partial C(t,x)}{\partial t} + \frac{\rho_b}{\theta}\frac{\partial C^*(t,x)}{\partial t} = D\frac{\partial^2 C(t,x)}{\partial x^2} - U_{tot}\frac{\partial C(t,x)}{\partial x} - \lambda C(t,x) - \lambda^*\frac{\rho_b}{\theta}C^*(t,x)$$

$$U_{tot} = U + U_s$$

Colloid attachment onto the solid matrix

(*Sim and Chrysikopoulos*, 1998)

$$\frac{\rho_b}{\theta}\frac{\partial C^*(t,x)}{\partial t} = k_c C(t,x) - k_r\frac{\rho_b}{\theta}C^*(t,x) - \lambda^*\frac{\rho_b}{\theta}C^*(t,x)$$

Initial and boundary conditions

$$C(0,x) = 0$$

$$-D\frac{\partial C(t,0)}{\partial x} + U_{tot}C(t,0) = \begin{cases} U_{tot}C_0 & 0 < t \le t_p \\ 0 & t > t_p \end{cases}$$

$$\frac{\partial C(t,\infty)}{\partial x} = 0$$

Analytical solution

(Sim and Chrysikopoulos, 1998)

$$C(t,x)=\begin{cases}\Omega(t,x) & 0<t\le t_p\\ \Omega(t,x)-\Omega(t-t_p,x) & t>t_p\end{cases}$$

$$\Omega(t,x)=\frac{C_0U_{tot}}{D^{1/2}}\exp\left[\frac{U_{tot}x}{2D}\right]\left\{\int_0^t\int_0^\tau He^{-H\tau}J_0\left[2\left(B\xi(\tau-\xi)\right)^{1/2}\right]\right.$$
$$\cdot\left\{\frac{1}{(\pi\xi)^{1/2}}\exp\left[\frac{-x^2}{4D\xi}+\left(H-A-\frac{U_{tot}^2}{4D}\right)\xi\right]\right.$$
$$-\frac{U_{tot}}{2D^{1/2}}\exp\left[\frac{U_{tot}x}{2D}+(H-A)\xi\right]$$
$$\left.\left.\cdot\ \mathrm{erfc}\left[\frac{x}{2(D\xi)^{1/2}}+\frac{U_{tot}}{2}\left(\frac{\xi}{D}\right)^{1/2}\right]\right\}d\xi\,d\tau\right.$$
$$+e^{-Ht}\int_0^t J_0\left[2\left(B\xi(t-\xi)\right)^{1/2}\right]$$
$$\cdot\left\{\frac{1}{(\pi\xi)^{1/2}}\exp\left[\frac{-x^2}{4D\xi}+\left(H-A-\frac{U_{tot}^2}{4D}\right)\xi\right]\right.$$
$$-\frac{U_{tot}}{2D^{1/2}}\exp\left[\frac{U_{tot}x}{2D}+(H-A)\xi\right]$$
$$\left.\left.\cdot\ \mathrm{erfc}\left[\frac{x}{2(D\xi)^{1/2}}+\frac{U_{tot}}{2}\left(\frac{\xi}{D}\right)^{1/2}\right]\right\}d\xi\right\}.$$

$A=k_c+\lambda,$

$B=k_ck_r\theta/\rho,$

$H=(k_c\theta/\rho)+\lambda^*,$

J_0 = Bessel function (first-kind of zeroth-order)

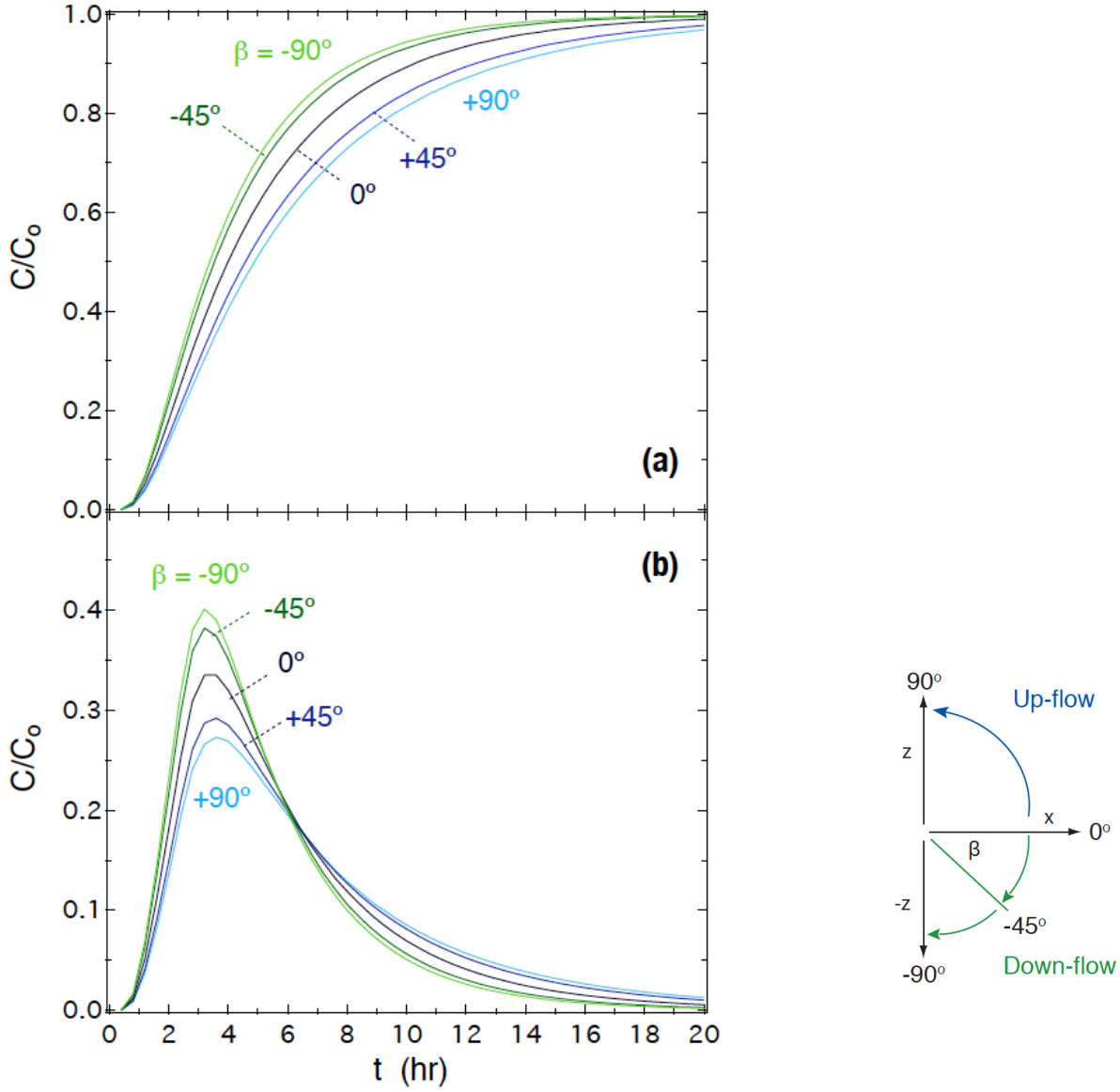

Figure B3. Simulations of normalized colloid break through curves for packed columns with various orientations and flow directions under: (a) continuous, and (b) broad pulse inlet boundary conditions.

Materials & methods

Columns: diameter = 2.5 cm
length = 30 cm
packed with glass beads (d_c = 2 mm)
columns were placed horizontally (0°),
vertically (90°),
inclined (45°).

Clays: kaolinite (KGa-1b), specific surface area of 10.1 m^2/g,
d_p=843±126 nm
montmorillonite (STx-1b), specific surface area of 82.9 m^2/g ,
d_p=1187±381 nm
C_o =10^7 to 10^{13} particles/mL
detection by UV-vis spectrophotometer

Tracer: bromide in the form of NaBr (10^{-5} M)
ion chromatography

Unfavorable to deposition transport conditions (pH=7, I_s=0.1mM).
Experimental data fitted with ColloidFit.

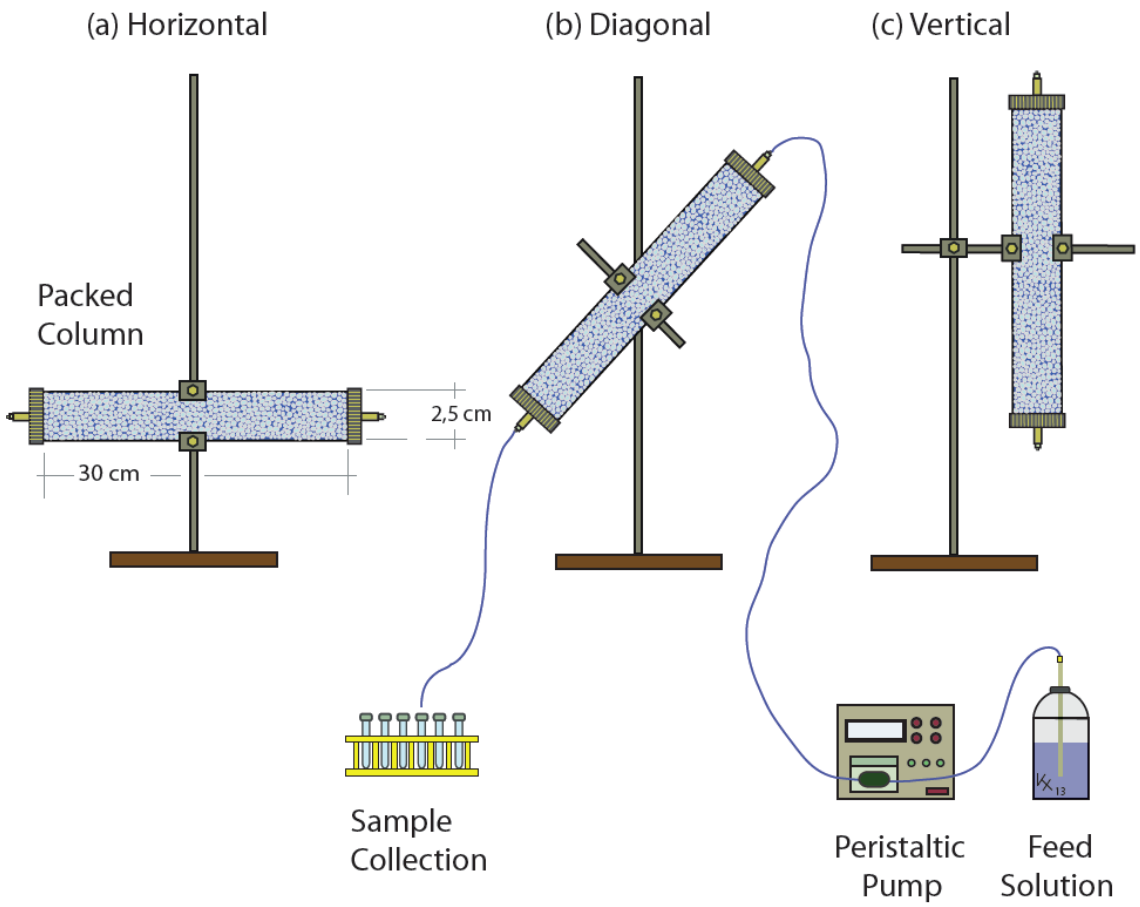

Figure B4. Experimental setup showing the various column arrangements: (a) horizontal, (b) diagonal, and (c) vertical.

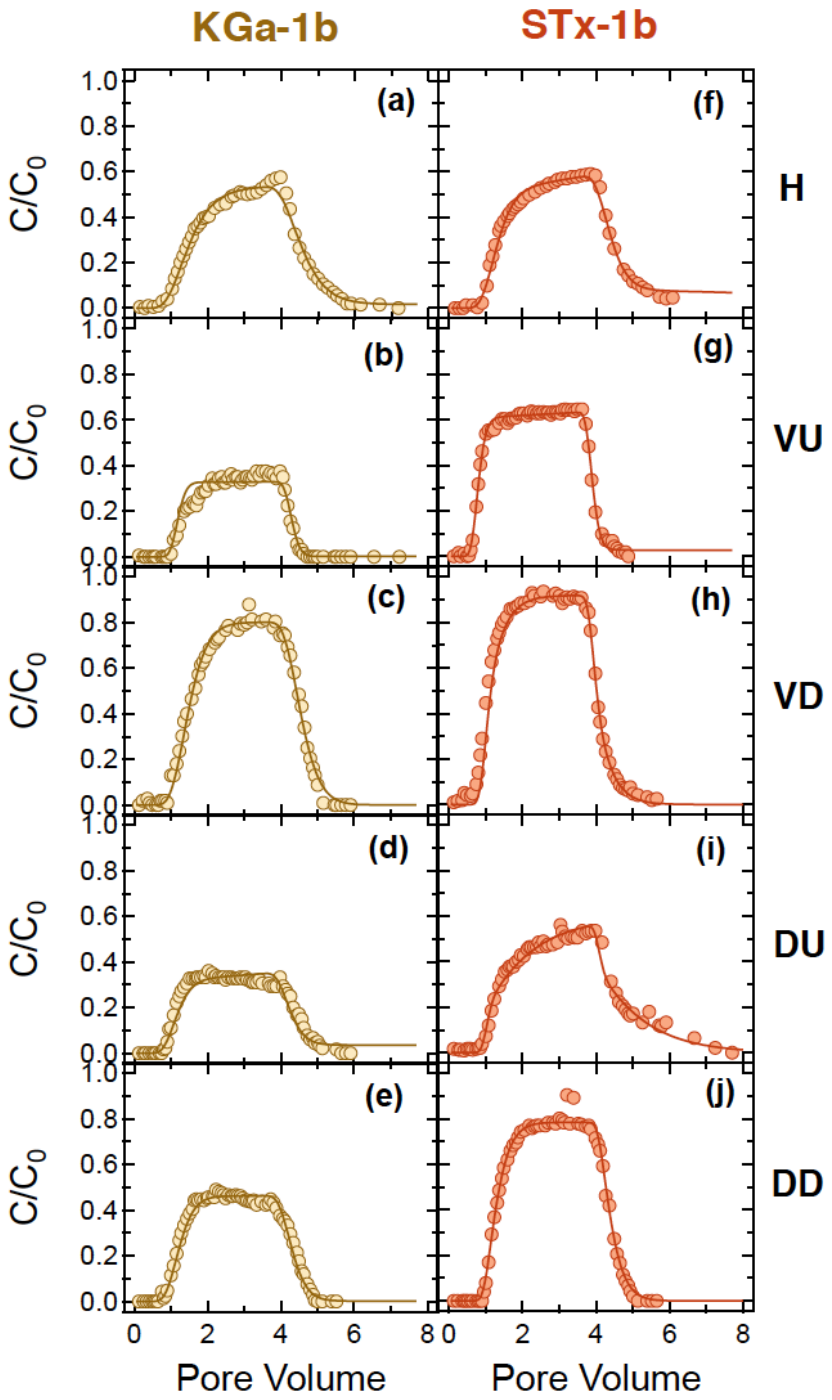

kaolinite: KGa-1b
montmorillonite: STx-1b

H: horizontal
VU: vertical up-flow
VD: vertical down-flow
DU: diagonal up-flow
DD: diagonal down-flow

Figure B5. Experimental data (symbols) and fitted model simulations (curves)

Table 1. Fitted U_{tot} and estimated mass recoveries

Exp. No	Flow Direction*	U_{tot} (cm/min)	U_s (cm/min)	M_r (%)	$M_{1(c)}/M_{1(t)}$
KGa-1b					
1	H	0.73741±0.0018	–	53.5	1.19
2	VU	0.73841±0.0008	-0.00159	32.6	1.05
3	VD	0.74193±0.0009	0.00193	79.5	1.12
4	DU	0.73474±0.0015	-0.00526	37.6	1.07
5	DD	0.74330±0.0016	0.00330	47.9	1.05
STx-1b					
6	H	0.73895±0.0004	–	58.6	1.16
7	VU	0.73827±0.0016	-0.00174	65	0.89
8	VD	0.74219±0.0013	0.00219	93.8	1.01
9	DU	0.73264±0.0023	-0.00736	61.5	1.31
10	DD	0.74439±0.0026	0.00438	83.1	1.06
Tracer					
	H	0.74016±0.0001	–	100	
	VU, VD	0.73985±0.0002	–	100	
	DU, DD	0.73995±0.0001	–	100	

* H-horizontal,
VU-vertical up-flow
VD-vertical down-flow
DU-diagonal up-flow
DD-diagonal down-flow

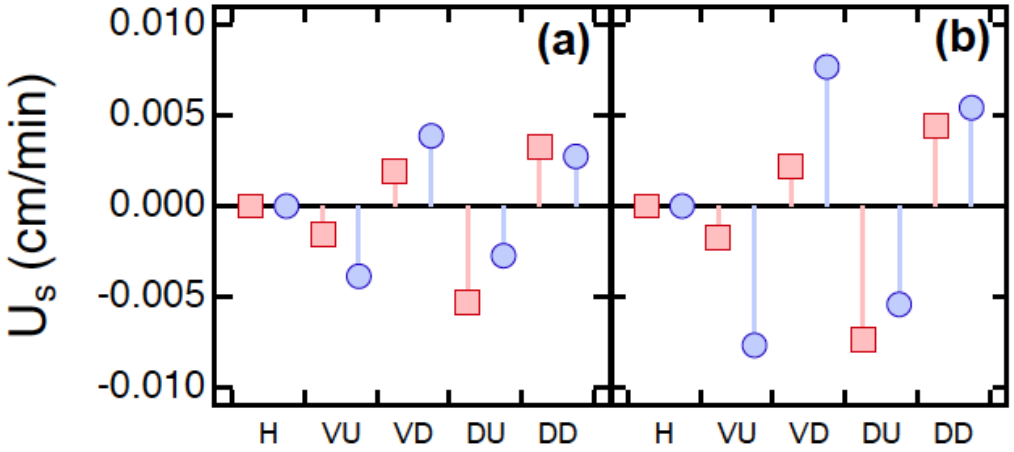

Figure B6. Comparison between theoretically estimated (circles) and fitted (squares) U_s values for: (a) KGa-1b, and (b) STx-1b. $U_s<0$ for up-flow and $U_s>0$ for down-flow experiments.
Here: H-horizontal, VU-vertical up-flow, VD-vertical down-flow,
DU-diagonal up-flow, DD-diagonal down-flow.

Results: Gravity effects

- Flow direction influences colloid transport in porous media.
- Gravity is a significant driving force for colloid deposition.
- Mass recoveries are higher for vertical-down than diagonal-down flow direction.
- Particle deposition is greater for up-flow than for down-flow direction.

Summary

- Dispersivity, typically considered only a property of the medium, is also a function of colloid size.
- Contrary to earlier results, colloid dispersivity increases with increasing colloid diameter.
- Gravity effects can be important and should not be neglected in colloid transport models.

Thank you for your attention

Transp Porous Med (2013) 100:377–392
DOI 10.1007/s11242-013-0220-4

Suspended Particles Transport and Deposition in Saturated Granular Porous Medium: Particle Size Effects

Lyacine Bennacer · Nasre-Dine Ahfir · Abderrazak Bouanani · Abdellah Alem · Huaqing Wang

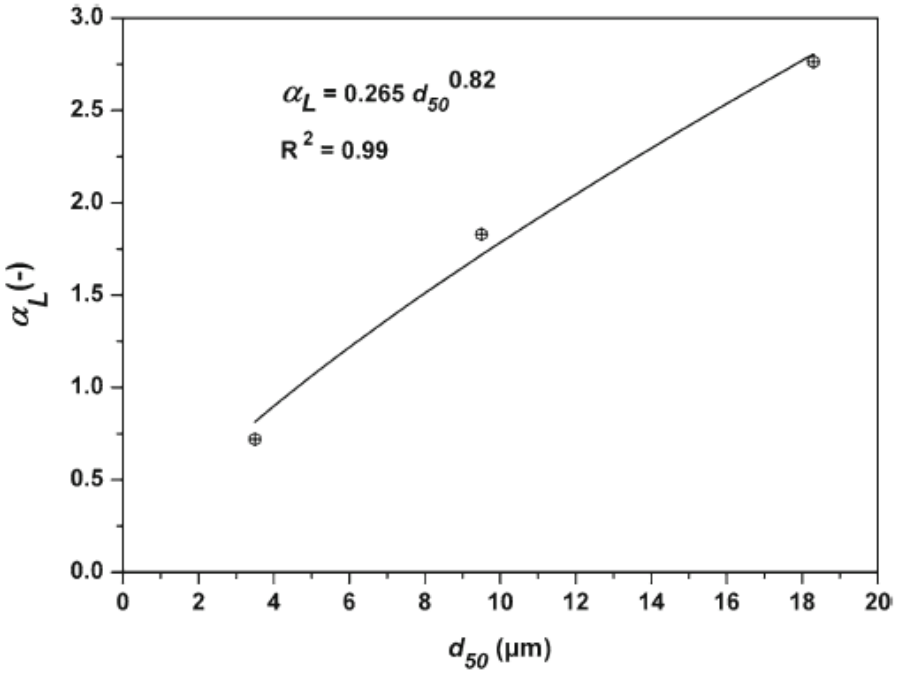

Longitudinal dispersivity (α_L) as a function of the d_{50} of calibrated populations (3.5, 9.5, and 18.3 µm)

Advances in Water Resources 62 (2013) 303–316

Contents lists available at ScienceDirect

Advances in Water Resources

journal homepage: www.elsevier.com/locate/advwatres

A mathematical and computational study of the dispersivity tensor in anisotropic porous media

Yuan Liu*, Peter K. Kitanidis

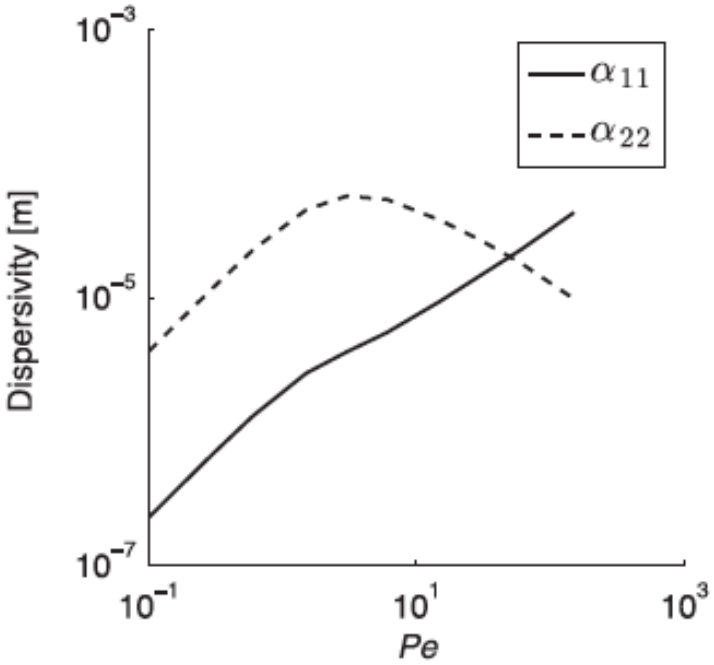

Fig. 3. Longitudinal (α_{11}) and transverse dispersivities (α_{22}) of the 2-D isotropic medium.

Colloids and Surfaces B: Biointerfaces 92 (2012) 74–83

Contents lists available at SciVerse ScienceDirect

Colloids and Surfaces B: Biointerfaces

journal homepage: www.elsevier.com/locate/colsurfb

Attachment of bacteriophages MS2 and ΦX174 onto kaolinite and montmorillonite: Extended-DLVO interactions

Constantinos V. Chrysikopoulos*, Vasiliki I. Syngouna

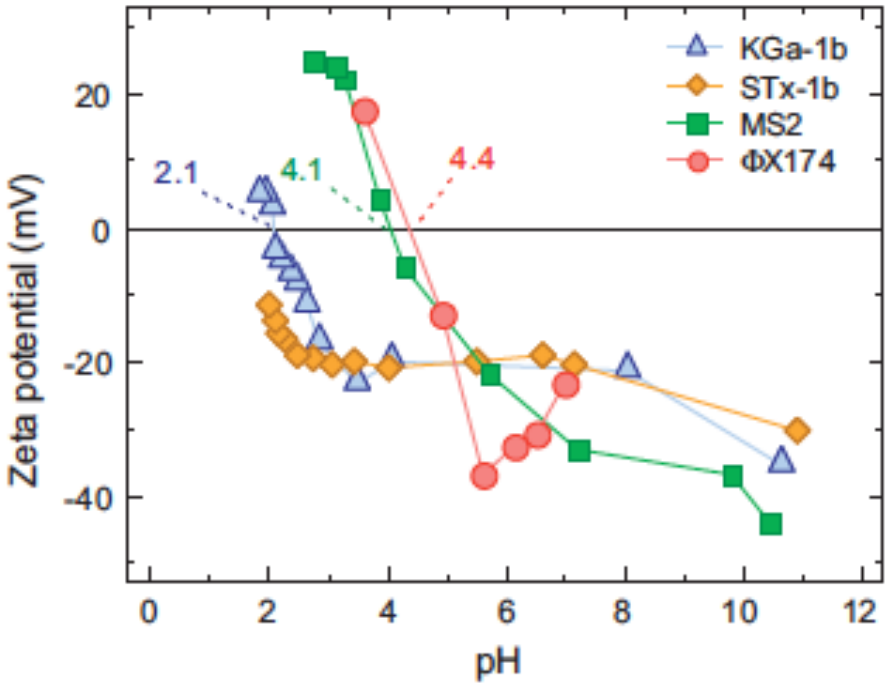

Fig. 5. Zeta potential as a function of solution pH for KGa-1b (triangles), STx-1b (diamonds), MS2 (squares), and ΦX174 (circles) in ddH_2O at 25 °C.

Previous studies

Early breakthrough of colloids as compared to conservative tracers

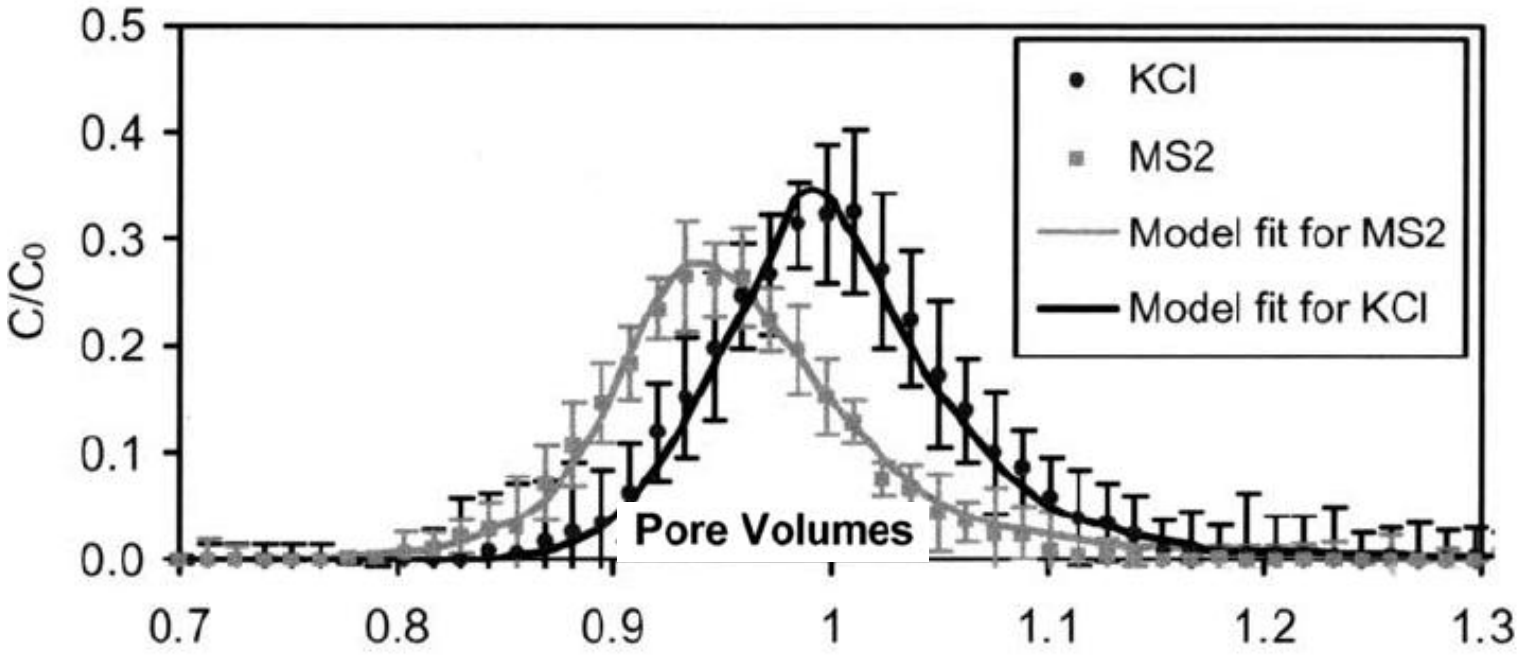

*

"Larger colloids are restricted by the size exclusion effect from sampling all paths, and therefore they tend to disperse less and move in the faster streamlines, if they are not filtered out."

* Keller, A. A., S. S. Sirivithayapakorn, C.V. Chrysikopoulos, *Water Resour. Res.*, 40, W08304, 2004.